Available online at www.sciencedirect.com
SCIENCE DIRECT
Europ. J. Agronomy 25 (2006) 138–154
European Journal of Agronomy
www.elsevier.com/locate/eja

Modelling protein content and composition in relation to crop nitrogen dynamics for wheat

Pierre Martre [a,*], Peter D. Jamieson [b], Mikhail A. Semenov [c], Robert F. Zyskowski [b], John R. Porter [d], Eugène Triboi [a]

[a] *INRA, UR874 Agronomie, 234 Avenue du Brezet, Clermont-Ferrand F-63 100, France*
[b] *New Zealand Institute for Crop and Food Research Ltd., Private Bag 4704, Christchurch, New Zealand*
[c] *Biomathematics & Bioinformatics, Rothamsted Research, Harpenden, Hertfordshire AL5 2JQ, UK*
[d] *Department of Agricultural Sciences, Royal Veterinary and Agricultural University, 2630 Taastrup, Denmark*

Abstract

Protein concentration and composition are key components of the end-use value for wheat (*Triticum aestivum* L.) grain. Although the qualitative composition of the grain is genetically determined, the quantitative composition is significantly modified by growing conditions, and there are important management × genotype × environment interactions. We recently reported a model of grain N accumulation and partitioning for wheat grain. The main assumptions made in this model are: (1) the accumulation of structural/metabolic proteins (albumins-globulins and amphiphils) is sink-driven and is a function of temperature; (2) the accumulation of storage proteins (gliadins and glutenins) is supply limited; (3) on the one hand the allocation of structural/metabolic proteins between albumin-globulin and amphiphilic protein fractions and on the other hand the allocation of storage protein between gliadin and glutenin fractions during grain growth is constant. A modified version of this grain model has been coupled with a revised version of the wheat simulation model Sirius99, allowing us to analyze the interactions between the vegetative sources and the reproductive sinks for N at the crop level. The main modifications to Sirius99 concerned the post-anthesis N uptake and remobilisation. After anthesis, the potential rate of crop N uptake was assumed to decrease linearly with accumulated thermal time, and the actual rate of N uptake was limited by the capacity of the stem to store accumulated N. During grain filling the daily rate of N transfer to grain was calculated daily according to the current crop N-status. The coupled model (*SiriusQuality*1) simulated dynamics of total grain N and of the different grain protein fractions reasonably well. At maturity, measured total grain N ranged from 0.56 to 1.32 mg N grain^{-1}, and the observed and simulated total grain N were well correlated ($r^2 = 0.82$, slope = 1.08) with a mean error of prediction of 0.11 mg N grain^{-1}. The simulated kinetics of crop N accumulation and stem N were closer to the observations with *SiriusQuality*1 than with Sirius99, in particular during the reproductive stage. At maturity, simulated and observed quantities of albumins-globulins were poorly correlated ($r^2 = 0.02$). Over the 18 experimental cases studied here, the quantity of storage proteins varied more than three-fold, and the observed and simulated quantities of gliadins and glutenins were well correlated ($r^2 = 0.79$ and 0.72, respectively). The simulations of total N and storage proteins accumulation provided by *SiriusQuality*1 confirmed that accumulation of grain N is overall source- rather than sink-regulated, at least under non-luxury N conditions. *SiriusQuality*1 provides a simple mechanistic framework that explains environmental effects on grain protein concentration and composition. The next step is to incorporate genetically related model parameters that will portray genotypic differences in protein concentration and composition.

Keywords: Wheat quality; Crop simulation model; Gliadins; Glutenins; *SiriusQuality*1; *Triticum aestivum* L

1. Introduction

Proteins are the most important components of wheat (*Triticum aestivum* L.) grains governing end-use quality (Weegels et al., 1996). Variations in both protein concentration and composition significantly modify flour end-use quality (Weegels et al., 1996; Lafiandra et al., 1999; Branlard et al., 2001). Although the qualitative composition of the grain is genetically determined, the quantitative composition (i.e., the ratio between the different protein fractions) is significantly modified by growing conditions, and there are significant genotype × environment interactions (Graybosch et al., 1996; Zhu and Khan, 2001).

Grain proteins can be divided into structural/metabolic and storage proteins (Shewry and Halford, 2002). Structural/metabolic proteins consist of albumin, globulin and

* Corresponding author. Tel.: +33 473 624 351; fax: +33 473 6244 57.
E-mail address: pmartre@clermont.inra.fr (P. Martre).

1161-0301/$ – see front matter © 2006 Elsevier B.V. All rights reserved.
doi:10.1016/j.eja.2006.04.007

amphiphilic proteins. Non-membrane amphiphilic proteins have been reported to have large effects on grain hardness and dough rheological properties (Dubreil et al., 1998). In wheat, storage proteins are divided into two broad fractions. These are gliadins, which are present as monomers, and glutenins, which form polymers. Gliadins and glutenin are the main components of gluten, which is the main contributor to the rheological and bread-making properties of wheat flour. Glutenins are mainly responsible for viscoelastic properties, and gliadins are important in conferring extensibility to dough (Branlard et al., 2001).

Structural/metabolic protein fractions accumulate mainly during the early phase of grain growth, when most endosperm cells are still dividing; whereas the accumulation of storage protein fractions occurs later when cell division has stopped and grain growth is due only to cell expansion (Stone and Nicolas, 1996; Triboï et al., 2003). The accumulation of the different protein fractions is highly asynchronous, implying that the protein composition of the grain changes during grain development. One consequence is that conditions that shorten the grain filling, such as high temperature or drought, affect the balance of protein fractions (Jamieson et al., 2001).

Moderately high temperatures of 25–32 °C have a positive effect on dough properties (Randall and Moss, 1990; Wrigley et al., 1994), and have been reported to lead to variation of the composition of the gliadin fraction (Daniel and Triboï, 2000). Analysis of the kinetics of accumulation of gliadins and glutenins in irrigated and non-irrigated fields did not show a significant effect of drought (Panozzo et al., 2001). Similarly, post-anthesis drought did not affect the rate of accumulation of SDS-soluble and SDS-insoluble glutenin polymers (Daniel and Triboï, 2002), however, post-anthesis drought shortened the period of grain filling before the onset of polymer insolubilisation (Daniel and Triboï, 2002). Additional N supply increases the total quantity of protein per grain at harvest ripeness and this is correlated with an increase in the quantity of gliadin and glutenin storage proteins for wheat (Pechanek et al., 1997; Wieser and Seilmeier, 1998) and hordeins for barley (Shewry et al., 2001). For wheat, increasing N supply usually leads to an increase of the percentage of gliadins while that of glutenins is not changed (Gupta et al., 1992; Jia et al., 1996); although, this is genotype dependent (Jia et al., 1996; Pechanek et al., 1997; Wieser and Seilmeier, 1998). The quantity per grain of albumins-globulins is scarcely influenced by N nutrition (Pechanek et al., 1997; Wieser and Seilmeier, 1998). Although temperature and water and N deficits have different effects on the rate and duration of accumulation of the different protein fractions, the process of N partitioning is not significantly affected by environmental conditions and at maturity the protein fraction composition depends mostly on the total quantity of N per grain (Triboï et al., 2003). This result was used to model the accumulation of structural/metabolic, glutenins and gliadins proteins using total grain N per grain as input variable (Martre et al., 2003). The main hypothesis of this model are: (1) the regulation by N sources of grain N accumulation applies only for the storage proteins, gliadin and glutenin fractions; (2) whereas accumulation of structural and metabolic proteins, albumin-globulin and amphiphilic fractions, is sink-regulated; (3) N partitioning between gliadins and glutenins is constant during grain development and unmodified by growing-conditions. Comparison of observed and simulated results of the accumulation of grain protein fractions under wide ranges of N fertilization, temperatures and irrigation showed a good agreement (Martre et al., 2003).

In the present study, a modified version of this grain model was coupled with the crop simulation model Sirius99 (Jamieson et al., 1998a; Jamieson and Semenov, 2000) allowing us to analyze the interactions between the vegetative sources and the reproductive sinks for N at the crop level. The post-anthesis rules of N remobilisation and uptake in Sirius99 were modified also to account for post-anthesis stem N accumulation, and the potential rate of transfer of N to the grain is now recalculated on a daily basis.

2. Model description

The *Sirius* model consists of submodels that describe phenological and canopy development, biomass accumulation and partitioning, including responses to shortages in the supply of soil water and N (Jamieson et al., 1998a). The canopy intercepts light and uses it to produce biomass at an efficiency (radiation use efficiency, RUE) calculated from temperature, water stress and the ratio of diffuse to direct radiation. The RUE in Sirius is independent of N supply because a major assumption is that the specific leaf N concentration is constant at 1.5 g N m^{-2} (Jamieson and Semenov, 2000). Hence, shortages of N limit leaf area, and hence light interception, rather than reduce RUE. Crop demand for N is set daily by the potential expansion of green area and increase in stem biomass. Stem biomass is calculated as the excess biomass after leaf biomass has been calculated assuming a fixed specific leaf mass of 45 g m^{-2}. Specific leaf mass is less than its maximum only early in the life of the crop if there is insufficient biomass for leaf tissue of that thickness. Stem biomass ceases accumulation at anthesis. Below we detail differences in the implementation of *SiriusQuality*1 used here from the originals described by Jamieson et al. (1998a) and Jamieson and Semenov (2000).

2.1. Canopy development

Canopy development was simulated using a model that describes the canopy as a series of leaf layers associated with individual mainstem leaves, and simulates tiller production through the potential size of any layer (Lawless et al., 2005). Green area consists of leaf laminae and all green surfaces (i.e., leaf sheaths, green stem and glumes), so that the summation of the surface area of each leaf layer per unit ground surface area gives the green area index. Area development in each leaf layer is described by a function that represents growth in the absence of resource limitations. Actual area achieved is calculated using simple limitation rules. New leaf area can be produced only if sufficient N is available from the soil or in the plant reserves (i.e., excess stem N) to maintain the fixed specific leaf N concentration. Potential for future growth is updated according to the current resource availability. This model assumes a constant small value for the potential maximum area for all leaves, until

the final leaf number per mainstem is calculated. The last four leaves are modelled as being larger and longer-lived than the earlier leaves. Linear increases in the maximum potential layer area and the layer lifetime with layer number are assumed. In the original version of this model (Lawless et al., 2005), the duration of constant area of the four last leaves ($T_{\max}^{\text{lag}}$; i.e., the period of thermal time between the end of leaf expansion and the beginning of leaf senescence) was rescaled after the final leaf number per mainstem was calculated, in order to synchronise the end of grain filling with the total senescence of the canopy. However, this reduced the duration of grain filling by 8–11 days under non-limiting N conditions, and $T_{\max}^{\text{lag}}$ was never reached, resulting in a significant underestimation of grain dry matter and N yield. In the present study, $T_{\max}^{\text{lag}}$ was set at 13 phyllochrons. It means that leaf senescence is driven by the translocation of N to the grains, and not by the leaves' life-span.

2.2. Leaf and stem dry matter and N assimilation and partitioning

Some variations were made from the original of Jamieson and Semenov (2000). Structural N concentration of stem was kept at 3 mg N g^{-1} DM, while leaf structural N was decreased to 6 mg N g^{-1} DM, from field measurements. Maximum stem N was set at 10 mg N g^{-1} DM, so that a maximum of 7 mg N g^{-1} DM was available for redistribution. Before anthesis crop N uptake is driven by the growth of the green area, and in contrast with Sirius99, in *SiriusQuality*1 crop N uptake is only limited by the capacity of the stem to store accumulated N.

In Sirius99, after anthesis the crop could accumulate N to satisfy grain N demand once the pool of remobilisable N had been depleted, but the accumulation of N in the vegetative tissues during that period was not modelled. In contrast, in *SiriusQuality*1 the stem was allowed to temporarily accumulate N after anthesis if its N concentration was less than its maximum and the only source of N for grains were the vegetative tissues (Section 2.3). The maximal net nitrate uptake rate of hydroponically grown wheat and barley (*Hordeum vulgare* L.) plants has been shown to increase until anthesis, then to decrease almost linearly with time, and correlates with the decrease of the root to shoot dry mass ratio (Oscarson et al., 1995). In *SiriusQuality*1, during the post-anthesis period, the senescence of the root system was accounted for by assuming that its potential rate of N uptake per unit ground area ($N_{\text{pot}}^{\text{uptake}}$, g N m^{-2} $days^{-1}$) decreases linearly with accumulated thermal time after anthesis to reach zero at the unconstrained end of grain filling:

$$N_{\text{pot}}^{\text{uptake}}(T) = N_{\max}^{\text{uptake}} \times \frac{D_{\text{gf}} - T}{D_{\text{gf}}}, \quad T > 0 \tag{1}$$

and

$$N^{\text{uptake}}(T) = \min(([N]_{\max}^{\text{stem}} - [N]_{\text{stru}}^{\text{stem}}) \times C_{\text{tot}}^{\text{stem}}(T), N_{\text{pot}}^{\text{uptake}}(T), N_{\text{av}}^{\text{soil}}(T)), \quad T > 0 \tag{2}$$

where $N_{\max}^{\text{uptake}}$ (g N m^{-2} $days^{-1}$) is the maximum daily rate of crop N uptake at anthesis, set at 0.4 g N m^{-2} $days^{-1}$ (Sinclair and Amir, 1992), D_{gf} (°C days) the duration of grain filling (starting at anthesis), T (°C days) the thermal time after anthesis, base 0 °C, $[N]_{\max}^{\text{stem}}$ and $[N]_{\text{stru}}^{\text{stem}}$ (g N g^{-1} DM) the maximum and structural stem N concentration, respectively, $C_{\text{tot}}^{\text{stem}}$ (g DM m^{-2}) the total stem dry mass per unit ground area and $N_{\text{av}}^{\text{soil}}$ (g N m^{-2}) is the mineral soil N available for the crop in the root zone per unit ground area.

2.3. Dry matter and N supply to grain

As in Sirius99, dry matter is supplied to grain assuming that from anthesis all new crop dry matter is available for transfer to the grain (Jamieson et al., 1998a). In addition, from the end of the grain cell division phase a fraction of the vegetative dry matter present at the end of cell division phase is available for the grain and is transferred at a potential rate set so that by the unconstrained end of grain filling all of the pool will have been transferred:

$$\begin{cases} C^{\text{supply}}(T) = \Delta C_{\text{tot}}^{\text{crop}}(T), & T < D_{\text{cd}} \\ C^{\text{supply}}(T) = \Delta C_{\text{tot}}^{\text{crop}}(T) + \gamma \times (C_{\text{tot}}^{\text{stem}}(T = D_{\text{cd}}) + C_{\text{tot}}^{\text{leaf}}(T = D_{\text{cd}})) \times \dfrac{\Delta T}{D_{\text{gf}} - D_{\text{cd}}}, & T \geq D_{\text{cd}} \end{cases} \tag{3}$$

where C^{supply} (g DM m^{-2} $days^{-1}$) is the potential daily rate of crop dry matter supply to grain, $\Delta C_{\text{tot}}^{\text{crop}}$ (g DM m^{-2} $days^{-1}$) the daily rate of accumulation of crop total dry matter, D_{cd} (°C days) the duration of the cell division phase, γ (dimensionless) the fraction of the vegetative total dry mass at the end of the cell division available for grain, set at 0.25 (Jamieson et al., 1998a), $C_{\text{tot}}^{\text{leaf}}$ (g DM m^{-2}) the total leaf dry matter and ΔT (°C) is the daily air temperature.

Nitrogen is supplied to grain assuming that all non-structural shoot N is available for transfer to grain. From anthesis to the end of the cell division phase, the daily flux of N transferred to grain (N^{supply}, g N m^{-2} $days^{-1}$) is set daily to match the daily demand of grain for structural/metabolic N. After the end of the cell division phase, N^{supply} is set daily so that all of the non-structural crop N would be transferred by the unconstrained end of grain filling:

$$N^{\text{supply}}(T) = (N_{\text{ns}}^{\text{stem}}(T) + N_{\text{ns}}^{\text{leaf}}(T)) \times \frac{\Delta T}{D_{\text{gf}} - D_{\text{cd}}}, \quad T > D_{\text{cd}} \tag{4}$$

where $N_{\text{ns}}^{\text{stem}}$ and $N_{\text{ns}}^{\text{leaf}}$ (g N m^{-2}) are the non-structural stem and leaf N, respectively.

Grain N is supplied from two sources. The first is excess stem N, including N released by natural leaf senescence. Should this source be insufficient then N is obtained by accelerating leaf senescence. N released from natural leaf senescence is computed daily as the amount of remobilisable N present in the leaves that senesce each day.

2.4. Grain number

In contrast with Sirius99, where grain number is not required to calculate the accumulation of grain dry matter and N, here grain number is a coupling variable between dry matter and N supply, defined at the crop scale, and the grain demand for structural/metabolic dry matter and N, defined at the grain scale. Grain number per unit area (G_{num}, grain m^{-2}) is also needed to partition structural/metabolic and storage protein fractions. Grain number was computed as in ARCWHEAT1 (Weir et al., 1984), where grain number is calculated from the ear mass at anthesis assuming one grain per 10 mg of ear dry mass. Ear dry mass (C_{tot}^{ear}, g DM m^{-2}) is accumulated starting 2.25 phyllochrons before anthesis. In line with the analysis presented by Jamieson et al. (1998a), during that period 50% of new crop dry matter, reduced by a water deficit factor for the day, is partitioned to the ear. A water deficit factor was introduced to make ear dry biomass accumulation more sensitive to water deficit than crop biomass accumulation (Jamieson et al., 1998a,b). The water deficit factor is calculated as the ratio of actual (E, mm $days^{-1}$, water supply limited) and potential (E_p, mm $days^{-1}$, energy limited) evapotranspiration (Jamieson and Ewert, 1999):

$$\Delta C_{tot}^{ear}(T) = \mu \times \Delta C_{tot}^{crop}(T) \times \left(\frac{E(T)}{E_p(T)}\right)^{s}, \quad -2.25P \le T < 0 \tag{5}$$

and

$$G_{num} = C_{tot}^{ear}(T = 0) \times \sigma \tag{6}$$

where μ (set at 0.5, dimensionless) is the partitioning coefficient of crop dry matter to ear, s (set at 0.8, dimensionless) is a scaling exponent of the transpiration efficiency, P ([°C days]$^{-1}$) the phyllochron and σ (equal to 100, grain g^{-1} ear) is the number of grains produced per gram of ear dry mass.

2.5. Accumulation of structural/metabolic and storage grain dry matter and N

The total grain dry matter (C_{tot}^{grain}, mg DM $grain^{-1}$) and N (N_{tot}^{grain}, mg N $grain^{-1}$) were divided into structural/metabolic (C_{stru}^{grain} and N_{stru}^{grain}) and storage (C_{sto}^{grain} and N_{sto}^{grain}) dry matter and N, respectively:

$$C_{tot}^{grain}(T) = C_{stru}^{grain}(T) + C_{sto}^{grain}(T) \tag{7}$$

and

$$N_{tot}^{grain}(T) = N_{stru}^{grain}(T) + N_{sto}^{grain}(T) \tag{8}$$

During the grain growth period, starting at anthesis, we distinguished an initial cell division phase and a grain-filling phase (Evers and Millar, 2002). During the cell division phase only C_{stru}^{grain} and N_{stru}^{grain} accumulate, and accumulation of C_{sto}^{grain} (i.e., starch) and N_{sto}^{grain} (i.e., gliadin and glutenin protein fractions) starts at the end of the cell division phase (Altenbach et al., 2003). We assumed that the accumulation of C_{stru}^{grain} and N_{stru}^{grain} are driven by grain demand (Martre et al., 2003). We set three hypotheses for simulating the daily demand of C_{stru}^{grain} (C_{stru}^{demand}, g DM $grain^{-1}$ $days^{-1}$). These were: (1) during the initial cell division phase, accumulation of C_{stru}^{grain} is exponential; (2) during the cell expansion phase, the rate of accumulation of C_{stru}^{grain} is determined by the quantity of C_{stru}^{grain} accumulated at the end of the cell division phase; (3) the end of accumulation of C_{stru}^{grain} coincides with the end of the DNA endoreduplication phase:

$$\begin{cases} C_{stru}^{demand}(T) = k_{cd} C_{stru}^{grain}(T)\Delta T, & T \le D_{cd} \\ C_{stru}^{demand}(T) = \dfrac{C_{stru}^{grain}(T = D_{cd})}{D_{cd}}\Delta T, & D_{cd} < T \le D_{er} \\ C_{stru}^{demand}(T) = 0, & T > D_{er} \end{cases} \tag{9}$$

where k_{cd} ([°C days]$^{-1}$) is the potential relative rate of accumulation of C_{stru}^{grain} during the cell division phase and D_{er} (°C days) is the duration of the DNA endoreduplication phase.

The actual daily flux of C_{stru}^{grain} was expressed as the minimum of C_{stru}^{demand} and the potential daily rate of crop dry matter supply to grain:

$$\Delta C_{stru}^{grain}(T) = \min\left(C_{stru}^{demand}(T), \frac{C^{supply}(T)}{G_{num}}\right) \tag{10}$$

Previous experimental results on barley suggest that N_{stru}^{grain} to C_{stru}^{grain} ratio ($\alpha_{N/C}$, g N g^{-1} DM) is constant during grain growth (Dreccer et al., 1997), thus the accumulation of N_{stru}^{grain} was calculated from that of C_{stru}^{grain}:

$$N_{stru}^{grain}(T) = \alpha_{N/C} \times C_{stru}^{grain}(T) \tag{11}$$

Experimental results on barley and maize indicates that accumulation of storage N is source regulated rather than sink driven (Tsai et al., 1980; Dreccer et al., 1997). Based on these results, we calculated the daily fluxes Δ of C_{sto}^{grain} and N_{sto}^{grain} as the difference between the daily potential rate of supply of dry matter and N and the daily rate of accumulation of structural/metabolic dry matter and N, respectively:

$$\Delta C_{sto}^{grain}(T) = \frac{C^{supply}(T)}{G_{num}} - \Delta C_{stru}^{grain}(T), \quad T > D_{cd} \tag{12}$$

and

$$\Delta N_{sto}^{grain}(T) = \frac{N^{supply}(T)}{G_{num}} - \Delta N_{stru}^{grain}(T), \quad T > D_{cd} \tag{13}$$

Thus, after the end of cell division grain N accumulates at a constant rate, in thermal time, until either the total senescence of the canopy, or the unconstrained end of grain filling, whichever occurs first. The unconstrained duration of grain filling is assumed to be under genetic control and constant in thermal time.

2.6. Partitioning of structural/metabolic and storage grain N

We initially assumed a constant partitioning of structural proteins between albumin-globulin and amphiphil fractions and of storage proteins between gliadin and glutenin fractions (Martre et al., 2003). This simple assumption gave close simulations of the quantity of the different protein fractions; it assumed constant albumin-globulin to amphiphil and gliadin to glutenin ratios. However, these ratios change during grain filling, because the accumulation of the different protein fractions are asynchronous (Triboï et al., 2003). The gliadin to glutenin ratio is a measure of molecular weight distribution or protein size, and determines the balances between dough viscosity and elasticity independently of total protein concentration and therefore affects dough rheological behaviour (Uthayakumaran et al., 1999). Thus here partitioning of N_{stu} between albumin-globulin ($N_{alb\text{-}glo}$, mg N grain^{-1}) and amphiphilic proteins (N_{amp}, mg N grain^{-1}), and of N_{sto} between gliadin (N_{gli}, mg N grain^{-1}) and glutenin proteins (N_{glu}, mg N grain^{-1}) during grain growth was assumed to follow an allometric power relation, allowing the ratios between protein fractions to vary.

$$\begin{cases} N_{alb\text{-}glo}(T) = \alpha_{alb\text{-}glo}(N_{stru}^{grain}(T))^{\beta_{alb\text{-}glo}} \\ N_{amp}(T) = N_{stru}^{grain}(T) - N_{alb\text{-}glo}(T) \end{cases} \quad (14)$$

and

$$\begin{cases} N_{glu}(T) = \alpha_{glu}(N_{sto}^{grain}(T))^{\beta glu} \\ N_{gli}(T) = N_{sto}^{grain}(T) - N_{glu}(T) \end{cases} \quad (15)$$

Phenology, evapotranspiration, root growth and soil water and nitrogen balances and distributions were calculated as in Sirius99 (Jamieson et al., 1998a; Jamieson and Semenov, 2000).

3. Materials and methods

3.1. Treatments

All experiments were carried out at Clermont–Ferrand, France (45°47′N, 3°10′E, 329 m elevation) with the winter wheat (*T. aestivum* L.) cv. Thésée. The experimental design, treatments, measurements and methodology are described in detail by Triboï et al. (2003), and are summarized in Table 1. Experiments were in two groups, semi-controlled environments and field.

In the semi-controlled environment experiments wheat was grown in 2 m^2 containers in controlled environment closed-top chambers under natural light. In 1993–1994, post-anthesis temperature was varied from −5 to +10 °C cf. ambient with some variation in timing, resulting in average daily post-anthesis temperature of 14.9–23.7 °C. In 1997–1998, warm and cool treatments were combined with the absence or presence of soil water deficit by supplying enough water to match evapotranspiration, or only 5–15% of that amount. One outdoor-controlled environment chamber was used per treatment. In order to study the dynamic accumulation of total N and protein fractions, three replicates each of 0.20 m^2 were collected every 3–8 days from anthesis to grain maturity. The number of plants and ears were determined, 20 averaged size plants were selected to determine leaves, stem, grain and chaff dry mass and N concentration.

In the field experiment, wheat was grown in an N-deficient soil, which was supplied with varying rates of N from both organic and inorganic sources. Three rates of inorganic N were supplied as ammonium-nitrate before anthesis: 0, 5 and 10 g N m^{-2}. At anthesis, each plot was split into three sub-plots to which 0, 3 or 15 g N m^{-2} were applied in the form of ammonium-nitrate. Samples of 0.22 m^2 were taken in each sub-plot at 0, 17, 36 and 50 days after anthesis. Three replicate sub-plots were used per N treatment.

3.2. Protein extraction and total N concentration determination

Grains were hand-threshed, and their dry mass was determined on sub-samples after oven drying at 70 °C to constant mass. The remaining grains were frozen in liquid N, freeze-dried and stored at 4 °C before analysis.

The protein fractions albumin-globulin, amphiphilic, gliadin and glutenin were sequentially extracted from whole meal flour (Triboï et al., 2003). Total grain N concentration for the different protein fractions were determined by the Kjeldhal method using a Kjeltec 2300 analyzer (Foss Tecator AB, Hoeganaes, Sweden). One sequential extraction and N concentration analysis was performed for each of the three independent replicates.

3.3. Criteria for model evaluation and comparison

Simulated and observed values were compared using mean squared deviation (MSD) and its square root (RMSD). MSD is the mean of the squared deviations around the 1:1 line in a plot of model simulation against measured values, and RMSD is the standard deviation of these deviations around the 1:1 line (Gauch et al., 2003). The MSD was partitioned into three components to gain further insight into model performance (Gauch et al., 2003): non-unity slope (NU), square bias (SB) and lack of correlation (LC). These MSD components, which add up to give MSD, represent different aspects of the overall deviation of the model simulations and have simple geometrical interpretation. NU reflects the rotation, SB the translation and LC the scattering (random error) around the 1:1 line. This analysis was used in complement of the classical least square linear regression.

4. Model calibration

Phenological development was not part of this study. Thus, the thermal time from sowing to emergence and the phyllochron were adjusted so that the simulated and observed emergence and anthesis dates matched. The thermal time from sowing to emergence was set at 175 and 125 °C days for the controlled environment closed-top chambers experiments in 1994 and 1998, respectively, and at 185 °C days for the field experiment. A phyllochron value of 94 °C days was used for the two

Table 1
Summary description of growing conditions in the field and semi-controlled condition experiments

Site	Treatment name	Sowing date	N fertilization (g N m^{-2})				From sowing to anthesis				From anthesis to mature harvest			
			Z21[a]	Z30[a]	Z39[a]	Z61[a]	Water supply (mm)		Global radiation (MJ m^{-2})	Average daily temperature (°C)	Water supply (mm)		Global radiation (MJ m^{-2})	Average daily temperature (°C)
							Precipitation	Irrigation			Precipitation	Irrigation		
Field														
	L0	13 December 1994	–	–	–	0	319	–	1701	8.7	61	–	1124	19.6
	L3	13 December 1994	–	–	–	3	319	–	1701	8.7	61	–	1124	19.6
	L15	13 December 1994	–	–	–	15	319	–	1701	8.7	61	–	1124	19.6
	M0	13 December 1994	–	–	5	0	319	–	1701	8.7	61	–	1124	19.6
	M3	13 December 1994	–	–	5	3	319	–	1701	8.7	61	–	1124	19.6
	M15	13 December 1994	–	–	5	15	319	–	1701	8.7	61	–	1124	19.6
	H0	13 December 1994	–	10	–	0	319	–	1701	8.7	61	–	1124	19.6
	H3	13 December 1994	–	10	–	3	319	–	1701	8.7	61	–	1124	19.6
	H15	13 December 1994	–	10	–	15	319	–	1701	8.7	61	–	1124	19.6
Semi-controlled conditions														
	−5	26 November 1993	3	10	10	10	327	60	1615	8.1	–	150	743	15.0
	0	26 November 1993	3	10	10	10	327	60	1615	8.1	67	135	990	18.6
	+5	26 November 1993	3	10	10	10	327	60	1615	8.1	–	145	522	22.4
	+5/+10	26 November 1993	3	10	10	10	327	60	1615	8.1	–	120	522	25.3
	+10/+5	26 November 1993	3	10	10	10	327	60	1615	8.1	–	145	522	24.1
	−5 W	04 November 1997	4	10	10	–	256	246	1726	8.2	–	235	1227	14.4
	−5D	04 November 1997	4	10	10	–	256	240	1726	8.2	–	13	1117	14.1
	+5 W	04 November 1997	4	10	10	–	256	247	1726	8.2	–	217	773	23.5
	+5D	04 November 1997	4	10	10	–	256	238	1726	8.2	–	43	773	23.5

All experiments were done with the winter bread wheat cultivar Thésée.
[a] Zadoks' scale: Z21, 1 tiller emerged; Z30, ear at 1 cm; Z39, flag leaf unfurled; Z61, anthesis.

controlled environment closed-top chambers experiments, and of 97 °C days for the field experiment. No detailed experiments to specify the vernalisation and daylength parameters within the *Sirius* framework had been done for the winter cultivar Thésée used in this study. Therefore, we assumed that the temperature response of vernalisation and daylength response for Thésée were similar to that for the cultivar Claire (Jamieson and Munro, 2000). This set of parameters gave a close simulation of the Haun index from emergence to anthesis (data not shown). The unconstrained duration of grain filling (from anthesis to the end of grain filling) was set at 750 °C days, as previously reported for the cultivar Thésée (Triboï and Triboï-Blondel, 2001). All the parameters of the canopy leaf layers model were set as in Lawless et al. (2005).

Using treatment 0 of the experiment in the controlled environment chambers, k_{cd} was estimated using reduced major axis regression (RMA) analysis (Niklas, 1994) as 8.44×10^{-3} °C days^{-1}, $\alpha_{alb\text{-}glo}$ and α_{glu} as 0.7242 and 0.6225 (dimensionless), respectively, and $\beta_{alb\text{-}glo}$ and β_{glu} as 0.9308 and 0.8980 mg N grain^{-1}, respectively. Using the same treatment, C_{stru}^{grain} ($T = 0$) was estimated as 1.33 mg DM grain^{-1}. For $\alpha_{N/C}$, we used the value of 20 mg N g^{-1} DM reported for barley (Dreccer et al., 1997). For D_{cd} we used the value of 250 °C days reported for grains of wheat (Gleadow et al., 1982; Singh and Jenner, 1982) and maize (Engelen-Eigles et al., 2000), and for D_{er} we used the value of 450 °C days reported for grains of maize (Engelen-Eigles et al., 2000).

The three sets of data used in this study for model evaluation are independent and have not been used for model calibration, except for the setting of some of the phenological parameters, which was done using treatments 0, L0 and −5, and of grain filling parameters, which was done using treatment 0 as described above.

5. Model evaluation

5.1. Total above-ground and grain biomass

*SiriusQuality*1 and Sirius99 gave similar simulations of above-ground and grain biomass accumulations (data not shown). In the field, simulated changes in above-ground and grain biomass matched well with observations for the low and medium pre-anthesis N treatments (treatments L and M; Fig. 1). For the high pre-anthesis N treatments (treatments H) both models overestimated biomass accumulation by ca. 31%. This overestimation was due mainly to an overestimation of pre-anthesis above-ground biomass accumulation, whereas growth rates of above-ground and grain biomass during grain filling were well

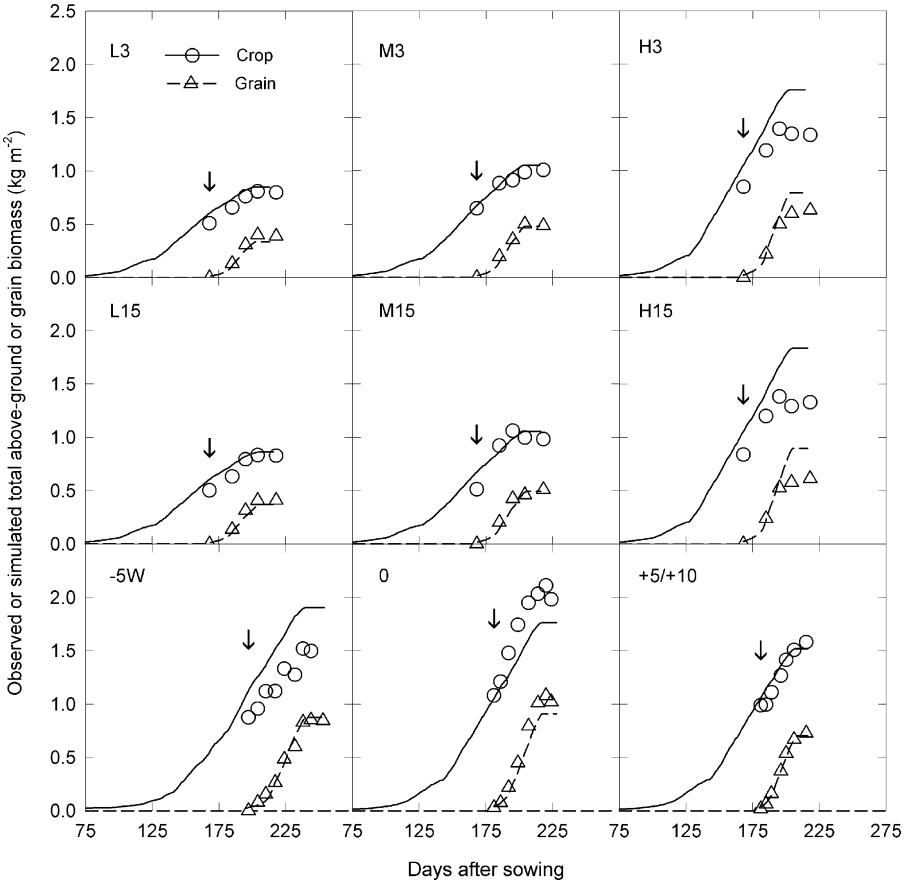

Fig. 1. Observed (symbols) and simulated (lines) total above-ground (circles) and grain (triangle) biomass vs. the number of days after sowing for crops of wheat (*Triticum aestivum* L.) grown in the field with different rates and timing of N fertilization (treatments L3, M3, H3, L15, M15 and H15), or under semi-controlled conditions with different post-anthesis temperatures (treatments −5 W, 0 and +5, and +5/+10). Treatments are denoted as outlined in Table 1. The vertical arrows indicate the anthesis date.

simulated. This was exemplified for high post-anthesis N supply (treatment H15), because the overestimation of anthesis above-ground biomass led to a delayed leaf senescence (data not shown) and thus to an overestimation of grain filling duration.

Under semi-controlled conditions, where average daily post-anthesis temperature ranged from 14.1 to 25.3 °C and post-anthesis water supply ranged from 13 to 235 mm simulations matched the grain biomass accumulation reasonably well, although the above-ground biomass was significantly overestimated for treatment −5 W and underestimated for treatment 0 (Fig. 1). In the latter case, the above-ground biomass around anthesis was predicted within 18% of the observed value, but the above-ground growth rate during grain filling was significantly underestimated.

*SiriusQuality*1 predicted duration of grain filling ranging from 465 °C days (for treatment L1) to 710–723 °C days (for treatments H15, −5, 0 and +5). Hence, even under non-limiting N supply the "genetic" duration of grain filling (set at 750 °C days) was never reached; the simulated duration of grain filling was determined by the dynamics of dry matter and N remobilisation and assimilation. Similarly, the duration of the canopy was never limited by the "genetic" parameter of the duration of constant area (T_{max}^{lag}). Instead leaf senescence was driven by the rate of N remobilisation.

When considering the 18N, temperature and watering treatments, observed grain yield varied more than three-folds, and observed and simulated grain yield were well correlated ($r^2 = 0.75$, slope = 0.91, d.f. = 17; Fig. 2A) with small squared bias and RMSD (Table 2). The largest component of the MSD for grain yield was LC—lack of correlation, which accounted for 87% of the overall error of prediction. In comparison, observed single grain dry mass varied only 1.3-folds. Simulations of single grain dry mass were relatively poor ($r^2 = 0.22$, slope = 0.62, d.f. = 17; Fig. 2B). In 12 of the 18 cases studied in this study, the model overestimated single grain dry mass, especially under the semi-controlled conditions. This overestimation was due to the simulation of grain number, which was underestimated in most of the cases (Fig. 3). Observed variations of grain yield in response to the environment were much higher than variations of single grain dry mass (Fig. 2), and grain yield variations were closely related to grain number variations ($r^2 = 0.80$, d.f. = 17). Because within the Sirius framework grain yield results from the bulk grain growth, independently of grain number, the model was able to simulate the yield variations quite well.

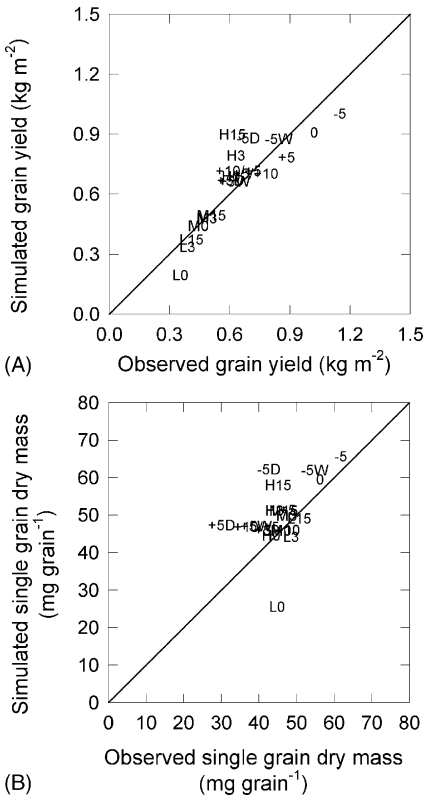

Fig. 2. Comparison of *SiriusQuality*1 simulations and observations for grain yield (A) and single grain dry mass (B) for crops of wheat grown either in the field with different rates and timing of N fertilization, or under semi-controlled conditions with different post-anthesis temperatures or watering regimes. Treatments are denoted as outlined in Table 1. The solid lines are $y = x$.

5.2. Total above-ground and grain N

In the nine N treatments of the field experiment and in the five temperature treatments of the 1993–1994 semi-controlled conditions experiment *SiriusQuality*1 and Sirius99 produced close simulations of above-ground N accumulation from sowing to anthesis, as illustrated Fig. 4. However, for the five temperature and drought treatments of the 1997–1998 semi-controlled conditions experiment, early in the crop life Sirius99 predicted a higher rate of leaf growth, and hence of crop biomass and N accumulations than *SiriusQuality*1. At anthesis, predicted crop N ranged from 4.2 to 16.0 g N m^{-2}, which compare favourably with the range of observed crop N (Table 2). As expected the differences between the two models were larger during the grain filling period. Although the two models gave comparable RMSDs for the cumulated post-anthesis crop N accumulation, the influence of the squared bias was two-times higher for Sirius99 than for *SiriusQuality*1 (Table 2). When considering the 18 experimental treatments, post-anthesis crop N accumulation represented 4–64% of mature crop N, compared with 5–61% and 4–47% for *SiriusQuality*1 and *Sirius99*, respectively. The most important difference between the two models was in the shape of the kinetics of post-anthesis N accumulation, which was more realistic with *SiriusQuality*1 than with Sirius99, especially under conditions of N shortage before anthesis (treatments L and M; Fig. 4). In Sirius99 grain N is supplied from three sources. The first one is excess stem N and N released by natural leaf senescence. If this is not sufficient then N is taken from the soil. Should these combined sources be insufficient then the required N is found by destruction of the GAI. Thus with Sirius99, even if some N is available in the soil, it is not used by the crop until the pool of labile N has been transferred to the grain. As a consequence, in the cases studied here post-anthesis crop N uptake was nil until 4–30 days after the beginning of linear grain filling. In contrast, with *SiriusQuality*1, post-anthesis N-uptake occurred during the whole grain filling period and the rate of N uptake decreased as the crop matured. *SiriusQuality*1 assumed

Table 2
Minimum and maximum observed values, root mean squared deviation (RMSD), mean squared deviation components: nonunity slope (NU), squared bias (SB) and lack of correlation (LC) and y-intercept, slope and correlation coefficient (r^2) from least square regression between simulated and observed values of GAI at anthesis, above-ground biomass and N at anthesis and maturity, grain dry mass and N yield, post-anthesis above-ground N accumulation, grain number, single grain dry mass and N, and grain protein concentration

	Anthesis			Maturity									
	GAI ($m^2\ m^{-2}$)	Above-ground biomass ($kg\ m^{-2}$)	Above-ground N ($g\ N\ m^{-2}$)	Above-ground biomass ($kg\ m^{-2}$)	Grain yield ($kg\ m^{-2}$)	Above-ground N ($g\ N\ m^{-2}$)	Grain N yield ($g\ N\ m^{-2}$)	Post-anthesis above-ground N accumulation ($g\ N\ m^{-2}$)	Grain number (10^3 grain m^{-2})	Single grain dry mass ($mg\ grain^{-1}$)	Single grain N ($mg\ N\ grain^{-1}$)	Grain protein concentration (mg protein g^{-1} DM)
Observed values												
Min	1.37	0.49	4.1	0.72	0.35	5.5	4.5	0.5	8.7	30.1	0.56	0.72
Max	5.50	1.13	18.8	2.09	1.15	29.1	24.2	10.1	20.2	61.7	1.32	1.51
RMSD	2.41	0.14	1.25	0.30	0.11	2.83	2.23	1.93	2.31	9.22	0.11	0.20
MSD components												
NU	1.61	1	1.4	77	16	15.4	2.3	0.9	81	31.9	0.003	0.03
SB	3.64	62	0.6	194	2	11.0	8.1	5.5	1593	17.3	0.001	0.09
LC	0.55	125	13.6	613	113	53.8	39.4	31.1	3668	35.8	0.007	0.27
Least square regression												
y-Intercept	0.31	0.27	1.50	0.43	0.07	4.13	2.22	1.39	3.09	21.82	−0.05	0.32
Slope	1.49	0.77	0.86	0.78	0.91	0.70	0.77	0.57	0.69	0.62	1.08	0.65
r^2	0.72	0.74	0.94	0.60	0.75	0.88	0.86	0.65	0.76	0.22	0.82	0.49

Data were obtained from the 18 N, temperature and drought treatments outlined in Table 1.

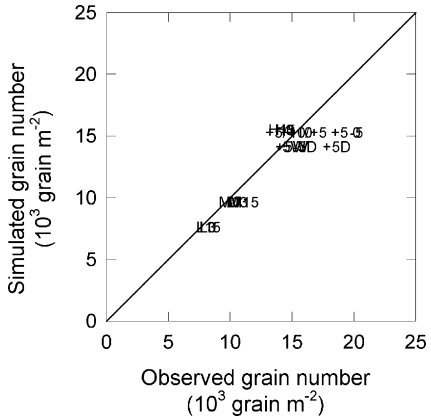

Fig. 3. Comparison of *SirusQuality*1 simulations and observations for grain number per square meter for crops of wheat grown either in the field with different rates and timing of N fertilization, or under semi-controlled conditions with different post-anthesis temperatures or watering regimes. Treatments are denoted as outlines in Table 1. The solid line is $y = x$.

that after anthesis the potential root N uptake decreases linearly with thermal time, but similar results were obtained when the capacity of the root system to uptake N was assumed to decrease linearly with GAI to reach zero at the same time as GAI (data not shown).

*SiriusQuality*1 provided close simulations of the rates and durations of grain N accumulation for most of the cases studied here (Fig. 5), the only exceptions were the treatments H15 and 0 in the field and semi-controlled conditions, respectively. In general *SiriusQuality*1 and Sirius99 gave similar kinetics of grain N accumulation; except for treatments L3 and L15, where Sirius99 significantly underestimated the rate of grain N accumulation whereas *SiriusQuality*1 matched the observed data (data not shown).

Maximum grain N yield and single grain N simulations were both well correlated with observations ($r^2 = 0.86$ and 0.82, respectively, d.f. = 17; Fig. 6), with RMSDs of 12% and 13% of the observed range of variations, respectively (Table 2). *SiriusQuality*1 simulated grain protein concentration with a RMSD of 0.19 mg protein g^{-1} DM with observations over a range from 0.72 to 1.51 mg protein g^{-1} DM (Table 2; Fig. 7). Seventy five percent of the MSD between observed and simulated protein concentration was due to the lack of correlation.

5.3. Accumulation of grain protein fractions

Under conditions of non-limiting soil N supply, the rate of accumulation of albumins-globulins and amphiphils increased by 63% and 50% when the average daily post-anthesis temperature was increased by 9 °C, respectively (Triboï et al., 2003). Post-anthesis drought had no significant effect on the rate of accumulation of the structural/metabolic protein fractions. Post-anthesis temperature and drought had similar effects on the duration of accumulation in days of albumins-globulins and amphiphils, which decreased by 16–53% (Triboï et al., 2003). The rate of accumulation of albumins-globulins and amphiphilics increased by a maximum of 60% for both protein fractions in response to N fertilization at anthesis for the L

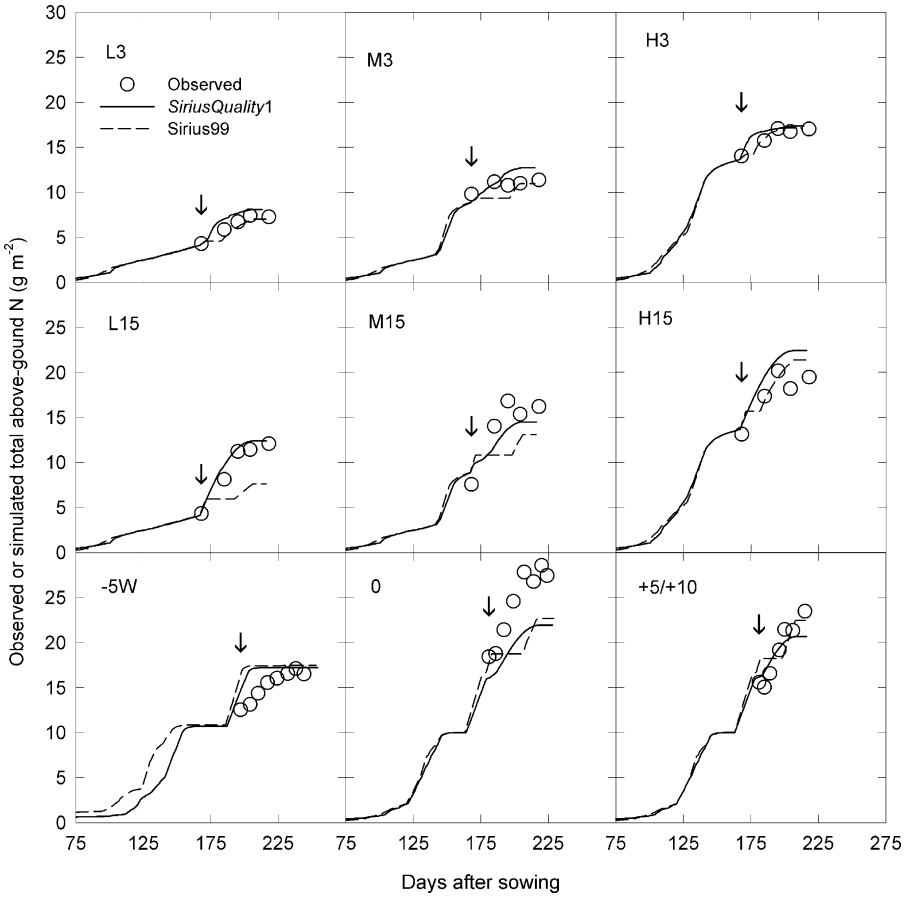

Fig. 4. Observed (symbols) and simulated (lines) total above-ground N vs. the number of days after sowing for crops of wheat grown in the field with different rates and timing of N fertilization (treatments L3, M3, H3, L15, M15 and H15), or under semi-controlled conditions with different post-anthesis temperatures (treatments −5 W, 0 and +5, and +5/+10). Treatments are denoted as outlined in Table 1. The vertical arrows indicate the anthesis date.

treatments, and by only 16–30% for the M and H treatments. Pre-anthesis N fertilization had no marked effect on the rate of accumulation of these protein fractions. The duration of accumulation of the structural/metabolic protein fractions was not significantly modified by N nutrition. Overall, these variations of the kinetics of accumulation of the structural/metabolic protein fractions were underestimated by *SiriusQuality*1 (Fig. 8).

The final quantity of albumins-globulins and amphiphilics varied by less than 1.6-fold in response to the N, temperature, drought treatments, with similar ranges of variations for the three environmental factors. *SiriusQuality*1 significantly underestimated the observed range of variations of the final quantity of the structural protein fractions, and simulated and observed final quantity of albumins-globulins and amphiphils were poorly correlated ($r^2 = 0.02$ and 0.07, respectively, d.f. = 17; Fig. 9A and B; Table 3).

Similarly to the response of structural protein fractions, the rate of accumulation of gliadins and glutenins increased by 35–60% in response to a 9 °C increase of the average daily post-anthesis temperature, whereas their duration of accumulation decreased by 42–52%. N nutrition had a much stronger effect on the kinetics of accumulation of the storage than on the structural/metabolic protein fractions. The rate of accumulation of gliadins increased about twice as much as that of glutenins in response to N nutrition. The duration of accumulation of gliadins and glutenins were not markedly modified by N nutrition, but it decreased in response to high post-anthesis temperature and drought. As for the structural/metabolic protein fractions, *SiriusQuality*1 mimicked quite well the effect of N, temperature and drought on the kinetics of accumulation of gliadins (Fig. 10). However, *SiriusQuality*1 overestimated the rate of accumulation of glutenins at the end of the grain filling period; this was especially obvious for the treatments H3, L15 and H15 presented in Fig. 10.

The correlations between simulated and observed final quantities of gliadins and glutenins were much better than for structural proteins (Fig. 9C and D), especially for gliadins whose quantity per grain was simulated with a RMSD of 10% of the observed range of variations (Table 3). The simulations of glutenins were skewed, high values were overestimated and low values underestimated.

Simulated variations of the gliadins to glutenins ratio due to the N treatments were reasonably well correlated with observed variations ($r^2 = 0.70$, d.f. = 8), but with quite a high RMSD (Fig. 11). However, simulated variations of the gliadins to glutenins ratio due to the temperature and drought treatments were poorly correlated with observations ($r^2 = 0.21$, d.f. = 8)

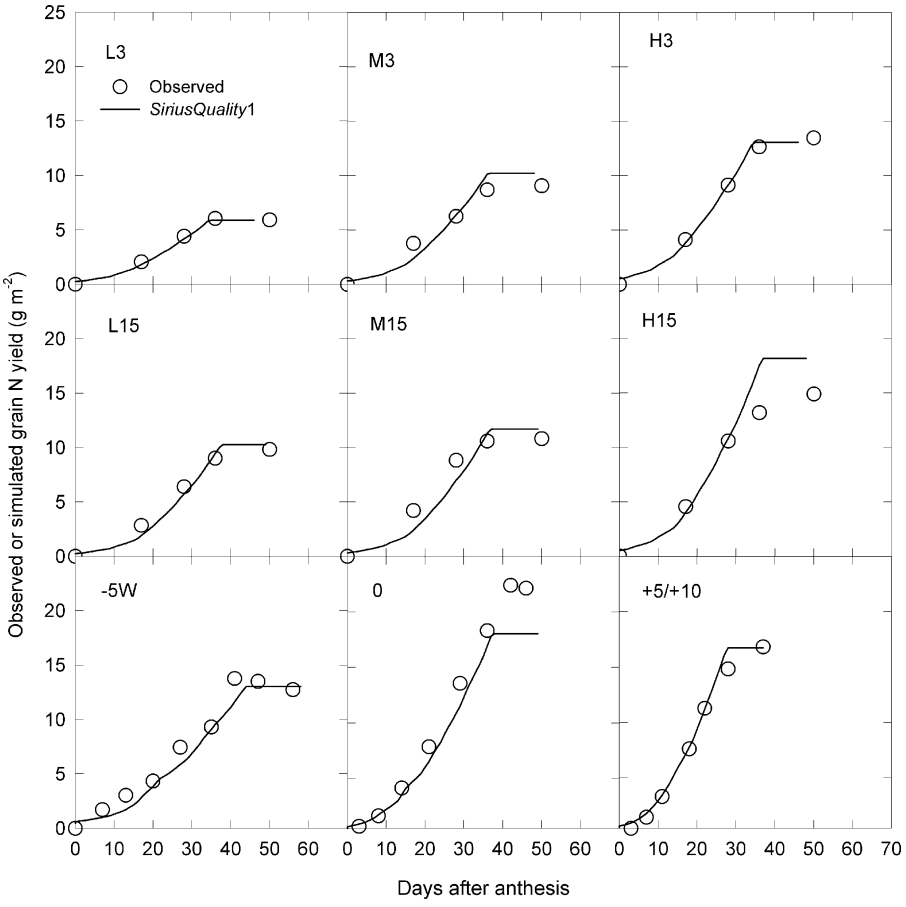

Fig. 5. Observed (symbols) and simulated (lines) grain N yield vs. the number of days after sowing for crops of wheat grown in the field with different rates and timing of N fertilization (treatments L3, M3, H3, L15, M15 and H15), or under semi-controlled conditions with different post-anthesis temperatures (treatments −5 W, 0 and +5, and +5/+10). Treatments are denoted as outlined in Table 1.

with an even higher RMSD (Table 3). In most cases, *SiriusQuality*1 underestimated the observed gliadins to glutenins ratio.

Grain number per unit ground area is the main coupling variable between Sirius and the model of grain protein accumulation and allocation (Martre et al., 2003). Thus, we assessed the contribution of the error of simulation of grain number per unit ground area on the accumulation of the protein fractions by running *SiriusQuality*1 with the observed grain number for each of the 18 experimental treatments. As expected, running *SiriusQuality*1 with the observed grain number did not modify the accumulation of structural/metabolic protein fractions, and the RMSD was not modified. However, running *SiriusQuality*1 with

Table 3
Minimum and maximum observed values, root mean squared deviation (RMSD), and *y*-intercept, slope and coefficient of correlation (r^2) from least square regression between simulated and observed values of the quantity of protein fractions per grain

	Albumins-globulins (mg N grain^{-1})	Amphiphils (mg N grain^{-1})	Gliadins (mg N grain^{-1})	Glutenins (mg N grain^{-1})	Gliadins to glutenins ratio (dimensionless)
Observed values					
Min	0.186	0.060	0.141	0.283	0.498
Max	0.380	0.122	0.315	0.508	0.727
RMSD	0.052	0.014	0.032	0.070	0.092
MSD components					
NU	0.0001	0.0000	0.0004	0.0017	0.0000
SB	0.0004	0.0000	0.0000	0.0020	0.0052
LC	0.0022	0.0002	0.0006	0.0013	0.0032
Least square regression					
y-Intercept	0.264	0.069	−0.026	−0.038	0.295
Slope	0.04	0.11	1.12	1.22	0.39
r^2	0.02	0.07	0.79	0.72	0.39

Data were obtained from the 18N, temperature and drought treatments outlined in Table 1.

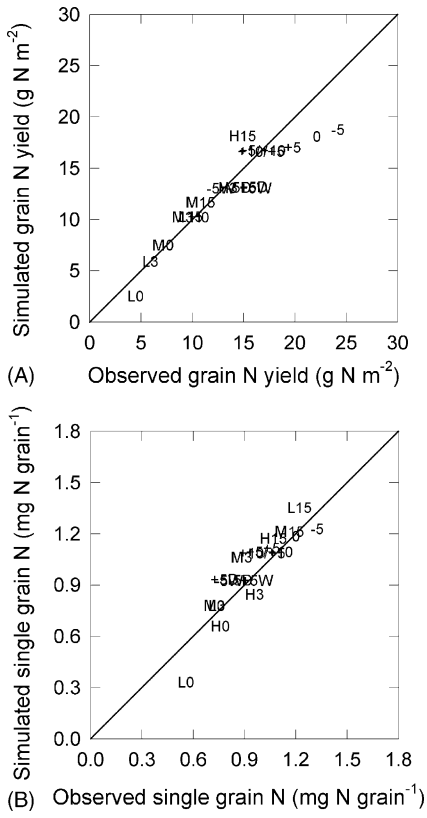

Fig. 6. Comparison of *SirusQuality*1 simulations and observations for grain N yield (A) and single grain N (B) for crops of wheat grown either in the field with different rates and timing of N fertilization, or under semi-controlled conditions with different post-anthesis temperatures or watering regimes. Treatments are denoted as outlined in Table 1. The solid lines are $y = x$.

the observed grain number decreased the RMSD for the quantity of glutenins per grain by 10%, but increased the RMSD for the quantity of gliadins per grain and of the gliadins to glutenins ratio by 40% and 30%, respectively. The difference in MSD between simulated and observed quantity of gliadins was mainly due to a three-fold decrease of the lack of correlation, whereas the changes of the MSD between simulated and observed quantity of glutenins and gliadins to glutenins ratio were mainly due to variations of the squared bias.

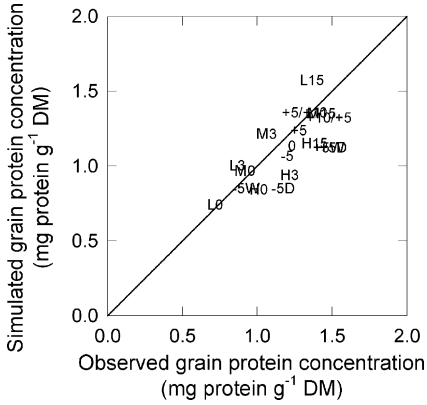

Fig. 7. Simulated vs. observed grain protein concentration for crops of wheat grown either in the field with different rates and timing of N fertilization, or under semi-controlled conditions with different post-anthesis temperatures or watering regimes. Treatments are denoted as outlines in Table 1. The solid line is $y = x$.

6. Discussion

Grain protein concentration and composition have long been recognized as major traits determining cereals end-use value. Several crop simulation models simulate the accumulation of grain dry mass and total N, and thus protein concentration (e.g., Porter, 1993; Brisson et al., 1998; Jamieson and Semenov, 2000; Asseng et al., 2002). However, no attempt has been made to model the accumulation of grain protein fractions yet. In this study, we tested new rules for post-anthesis N remobilisation and uptake and modified the wheat simulation model Sirius99 (Jamieson et al., 1998a; Jamieson and Semenov, 2000) to couple it with a modified model of grain protein accumulation and allocation (Martre et al., 2003). The simulation results supported the hypothesis that grain N accumulation is primarily source regulated, and that the synthesis of the main protein fractions is determined by the quantity of N per grain, and thus by the rate of N transfer to the grain. These results strongly suggest that genotype by environment interactions for grain protein composition reported earlier act mostly via variations of total N per grain, and thus, N availability and not via the regulation of protein synthesis in the grain.

There is an interesting contrast between the requirements for detail, and therefore the probable mechanisms, when comparing simulations of protein composition with the simulation of yield and total grain N. *SiriusQuality*1, in common with earlier versions of Sirius, simulates the accumulation of biomass and total N by the grain in bulk. In this case calculation of grain number at anthesis simply provides a method of calculating final grain size—it has no place in grain yield and total N calculation. There is obviously a close balance between grain numbers, the main yield component that varies when yield varies substantially, and the ability of the crop to fill them (Jamieson et al., 1998a,b). This ability is regulated by the survival of tillers and the resources held and captured by the leaves thereon. In contrast, we have shown that the simulation of grain protein composition does require an estimate of grain number, because composition appears to be regulated at the level of the individual grain (Martre et al., 2003; Triboï et al., 2003).

The errors in the simulation of grain number had no influence on the simulation of the quantity of structural/metabolic protein fractions per grain; this was expected since in the model their accumulation is driven by the grain demand for structural/metabolic protein, which was calculated on a per grain basis. Although grain number is the main coupling variable between Sirius and the model of grain protein accumulation and allocation, the error in the simulation of grain number appeared to have a surprisingly low effect on the overall error of simulation of grain storage proteins accumulation with *SiriusQuality*1. Additional errors in the estimation of the quantity of protein fractions are essentially due to the errors in the simulation of the end of grain filling.

A direct implication in the regulation of the synthesis of cereal storage proteins has been attributed to the presence of a con-

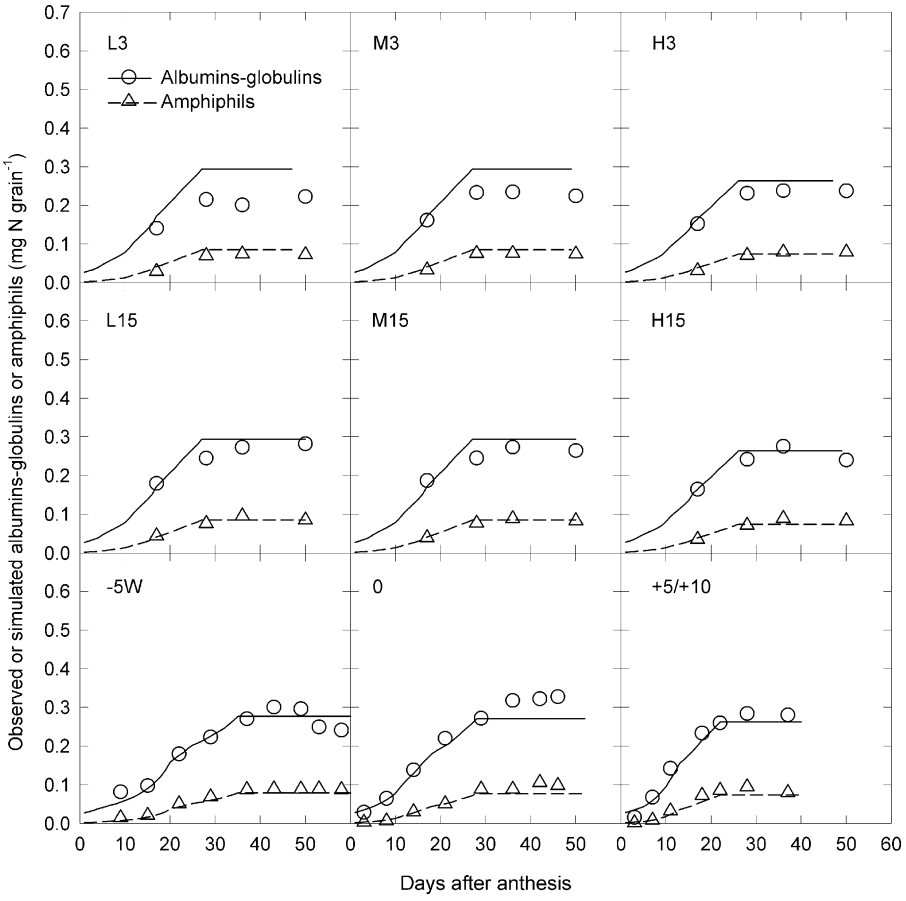

Fig. 8. Observed (symbols) and simulated (lines) quantities of albumins-globulins (circle) and amphiphilic (triangle) protein per grain vs. the number of days after anthesis for grains of wheat crops grown in the field with different rates and timing of N fertilization (treatments L3, M3, H3, L15, M15 and H15), or under semi-controlled conditions with different post-anthesis temperatures (treatments −5 W, 0 and +5, and +5/+10). Treatments are denoted as outlines in Table 1.

served bi-partite endosperm box in the promoter region of most of the cereal grain storage protein genes. This consists of two distinct protein-binding sites—the prolamin box recognized by transcription factors of the DNA with one finger (DOF) class (Vicente-Carbajosa et al., 1997), and the GNC4-like motif recognized by bZIP transcription factors of the Opaque2 family (Onate et al., 1999). The latter one has been shown to confer a strong and specific N response in grain of barley (Müller and Knudsen, 1993). The GNC-4 like motif acts as a negative element under low-N conditions, and as an enhancer under high N conditions for grains of barley (Hammond-Kosack et al., 1993; Müller and Knudsen, 1993). These elements are conserved in most of the grain storage protein promoter regions of cereal species (see ref. in Müller and Knudsen, 1993), and the involvement of bZIP and DOF class transcriptional factors in the regulation of grain storage protein genes seems to be conserved throughout the cereals (Hwang et al., 2004). Regulation of storage protein accumulation by such transcriptional regulation may explain why the synthesis of grain protein fractions is related to the quantity of N per grain and not to the quantity of N per square meter or to grain N concentration, as shown by regression analysis (P.M. Martre, unpublished results). It may also explain why similar relationships have been found for several cereal species between the quantity of total N and that of storage protein fractions (Bishop, 1928; Landry, 2002). These results suggest that the model presented here can probably also be used to describe the accumulation of structural/metabolic and storage proteins for other cereal species.

We made several important modifications in the way Sirius99 simulates post-anthesis crop N uptake and remobilisation. In *SiriusQuality*1, during the post-anthesis period, the senescence of the root system was accounted for by assuming that its potential rate of N uptake per unit ground area ($N_{\text{pot}}^{\text{uptake}}$) decreases linearly with accumulated thermal time after anthesis to reach zero at the unconstrained end of grain filling. N accumulated after anthesis was temporarily stored in the stem, up to its maximum storage capacity, before it was transferred to grain. The benefit of this modification is that the empirical parameter accelerating the daily flux of N transfer to grain (N^{supply}) was eliminated from Sirius99. In place of this calibrated coefficient, it was necessary only to recalculate N^{supply} daily. Thus all the empirical parameters or stress factors related crop N dynamic and deficiency in the earlier versions of Sirius (Jamieson et al., 1998a) have now been replaced by physiological parameters, which more closely match plant function. The shape of the simulated kinetics of post-anthesis crop N accumulation were more realistic for *SiriusQuality*1 than for Sirius99; and for at least one treatment (L15) the simulation of post-anthesis crop N accumulation

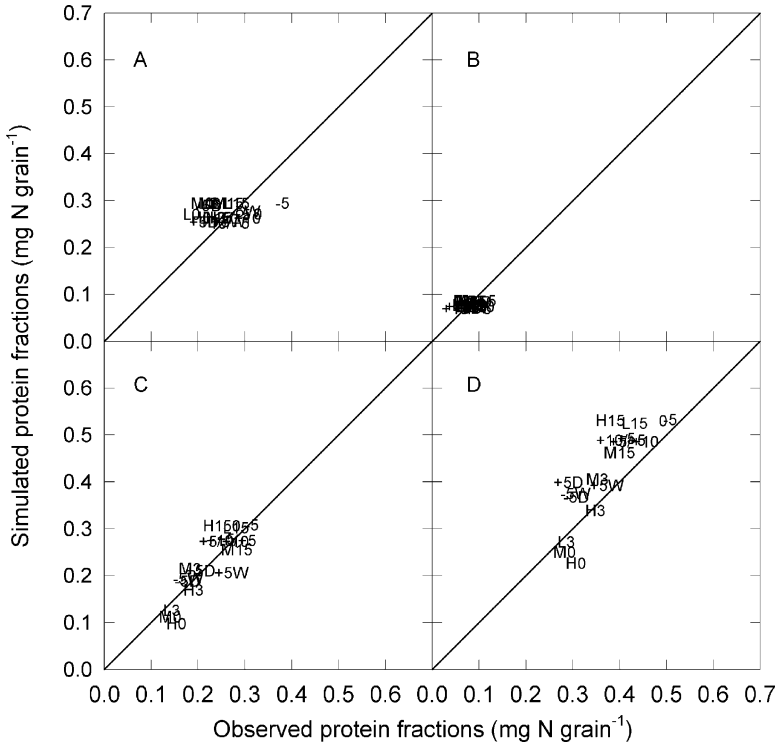

Fig. 9. Simulated vs. observed quantities of albumin-globulin (A), amphiphil (B), gliadin (C) and glutenin (D) protein fractions for mature grains of wheat crops grown either in the field with different rates and timing of N fertilization, or under semi-controlled conditions with different post-anthesis temperatures or watering regimes. Treatments are denoted as outlines in Table 1. The solid lines are $y = x$.

was much closer to the observed values for *SiriusQuality*1 than for Sirius99. Further stem N dynamics during the post-anthesis period compared much more favourably with observations.

In earlier versions of Sirius (Jamieson et al., 1998a; Lawless et al., 2005), leaf senescence was treated as a developmental process that occurred in thermal time so that leaves were completely senesced and had given up their N at the end of grain filling, which was determined by accumulated thermal time. N dynamics would accelerate senescence in low-N crops through premature senescence. In contrast, in *SiriusQuality*1 leaf senescence is assumed to be driven by N remobilisation, with N^{supply} recalculated each day according to the current crop N-status. Similarly the end of grain filling is assumed to be driven by post-anthesis N assimilation and N remobilisation. Indeed, the parameter defining the potential (genetic) duration of grain filling is implicated in: (1) the decrease of post-anthesis root N uptake capacity, (2) the rate of pre-anthesis dry matter remobilisation and (3) the rate of N remobilisation. Thus, in the model the end of grain filling is determined mainly by resource availability, but not by intrinsic grain characteristic or state variables. These assumptions imply that the primary driver of leaf senescence during grain filling is N remobilisation. However, they do not exclude feed-back regulations of the rate of N remobilisation, and thus of grain filling duration, by the grain, but they highlight the importance of the source in determined the rate and the duration of grain N accumulation.

During both the vegetative (Grindlay et al., 1995; Dreccer et al., 2000) and the reproductive (Bindraban, 1999) stage of wheat development leaf N has been shown to be non-uniform and vertical distribution of specific leaf N is determined by light interception. Sirius99 and *SiriusQuality*1 assume a uniform and constant distribution, with a specific leaf N of 1.5 g N m^{-2}. In spite of that we were able to simulate quite well the accumulation of above-ground and grain N. This means that although the vertical profile of specific N will vary substantially among crops with different histories and fertilization, the mean figure of 1.5 g N m^{-2} is robust. However, taking into account the vertical distribution of N might be important for simulating differences among genotypes (Dreccer et al., 1998).

*SiriusQuality*1 does not simulate all processes or properties. Differences in the bread-making quality observed from flour to flour are determined, in part, by a superimposition of the effects of protein concentration and gliadin to glutenin ratio (Uthayakumaran et al., 1999), and here we have attempted to deal with this part of the puzzle. However, these two effects are not sufficient to describe fully the structure–function relationship in dough, and further parameters, such as HMW-GS to LMW-GS ratio or molecular weight distribution of glutenin polymers need to be considered as well (Gras et al., 2001). Additionally, we do not simulate the observed variations of structural proteins well. We have assumed that they are sink-determined, but there may be other influences. *SiriusQuality*1 did not simulate the effect of N fertilization and post-anthesis water deficit on the accumulation of structural protein fractions. This may be due to the effect of N availability on grain demand for structural C and N, something that was not modelled.

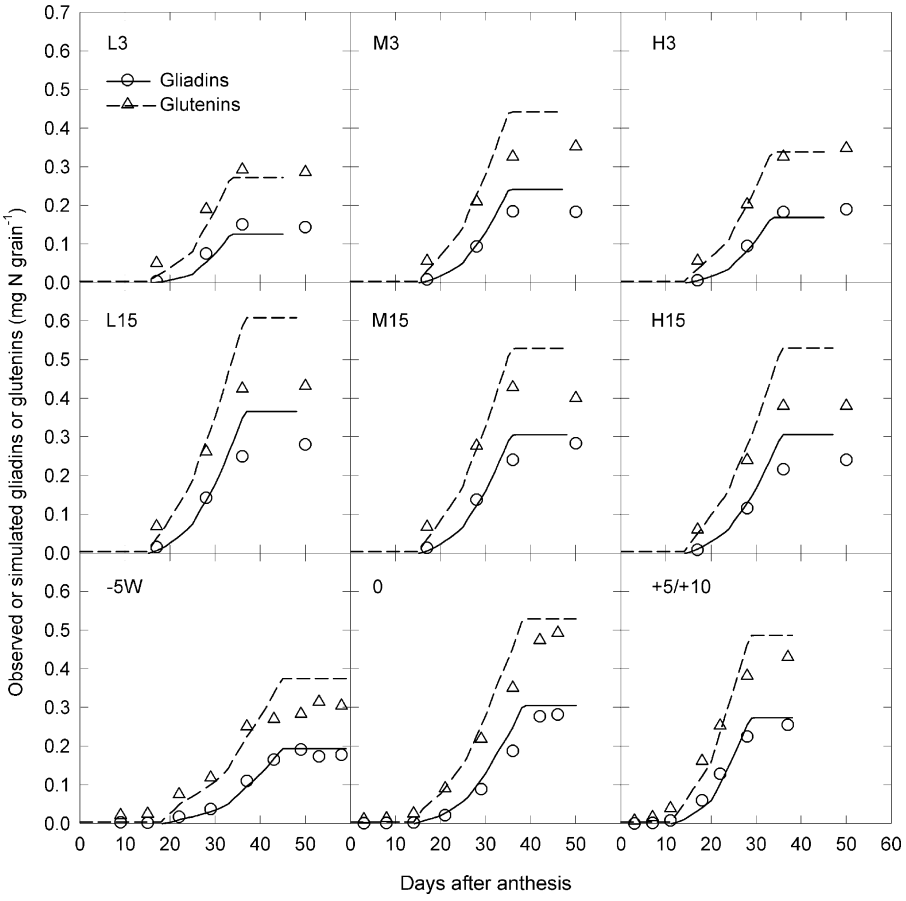

Fig. 10. Observed (symbols) and simulated (lines) quantities of gliadins (circle) and glutenins (triangle) per grain vs. the number of days after anthesis for grains of wheat crops grown in the field with different rates and timing of N fertilization (treatments L3, M3, H3, L15, M15 and H15), or under semi-controlled conditions with different post-anthesis temperatures (treatments −5 W, 0 and +5, and +5/+10). Treatments are denoted as outlines in Table 1.

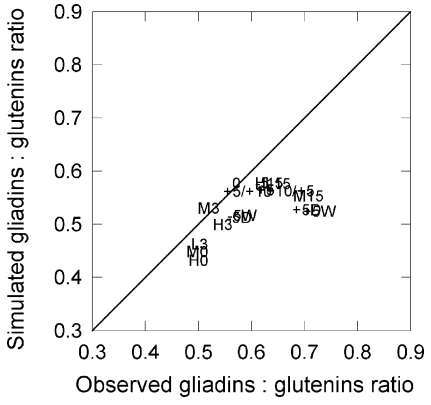

Fig. 11. Simulated vs. observed values of the gliadins to glutenins ratio for mature grains of wheat crops grown either in the field with different rates and timing of N fertilization, or under semi-controlled conditions with different post-anthesis temperatures or watering regimes. Treatments are denoted as outlined in Table 1. The solid line is $y = x$.

7. Conclusions

An essential point of this work has been to illustrate how to make quantitative predictions of crop quality based on simple but not simplistic physiological understanding. The simulations of total N and storage proteins accumulation provided by *SiriusQuality*1 confirm that accumulation of total grain N is source-regulated rather than sink-regulated, at least under non-luxury N conditions. *SiriusQuality*1 also gives a simple mechanistic framework that explains environmental effects on grain protein concentration and composition. Our assumptions that grain protein composition is a direct function of the total quantity of N per grain and that N partitioning is not affected by the growing conditions appeared to hold over a significant range of N fertilization and post-anthesis temperature and watering conditions. Although total grain N is determined at the crop scale and is largely independent of grain number, comparisons of observed and simulated quantity of the different grain protein fractions showed that grain protein partitioning is regulated at the grain scale rather than at the crop scale. We also provided a more mechanistic model of post-anthesis crop N uptake and remobilisation compared with Sirius99. An important point for the use of this model to analyze the genetic determinism of grain protein composition is the low number of parameters needed to model the accumulation of the different protein fractions. Moreover, all the parameters of *SiriusQuality*1 have simple physiological interpretations, and can by determined on a large number of genotypes, which could allow one to analyze their genetic variability and determinism.

Acknowledgements

The authors thank Prof. L.A. Hunt (University of Guelph, Canada) for overseeing the review process and Prof. J.H.J. Spiertz and two anonymous additional reviewers for valuable suggestions on how to improve the manuscript. Rothamsted Research receives grant-aided support from the Biotechnology and Biological Sciences Research Council of the United Kingdom.

References

Altenbach, S.B., DuPont, F.M., Kothari, K.M., Chan, R., Johnson, E.L., Lieu, D., 2003. Temperature, water and fertilizer influence the timing of key events during grain development in a US spring wheat. J. Cereal Sci. 37, 9–20.

Asseng, S., Bar-Tal, A., Bowden, J.W., Keating, B.A., Van Herwaarden, A., Palta, J.A., Huth, N.I., Probert, M.E., 2002. Simulation of grain protein content with APSIM-Nwheat. Eur. J. Agron. 16, 25–42.

Bindraban, P.S., 1999. Impact of canopy nitrogen profile in wheat on growth. Field Crops Res. 63, 63–77.

Bishop, L.R., 1928. The composition and quantitative estimation of barley proteins. J. Inst. Brewing 34, 101–118.

Branlard, G., Dardevet, M., Saccomano, R., Lagoutte, F., Gourdon, J., 2001. Genetic diversity of wheat storage proteins and bread wheat quality. Euphytica 119, 59–67.

Brisson, N., Mary, B., Ripoche, D., Jeuffroy, M.H., Ruget, F., Nicoullaud, B., Gate, P., Devienne-Barret, F., Antonioletti, R., Durr, C., Richard, G., Beaudoin, N., Recous, S., Tayot, X., Plenet, D., Cellier, P., Machet, J.M., Meynard, J.M., Delécolle, R., 1998. STICS: a generic model for the simulation of crops and their water and nitrogen balances. I. Theory and parameterization applied to wheat and corn. Agronomie 18, 311–346.

Daniel, C., Triboï, E., 2000. Effects of temperature and nitrogen nutrition on the grain composition of winter wheat: effects on gliadin content and composition. J. Cereal Sci. 32, 45–56.

Daniel, C., Triboï, E., 2002. Changes in wheat protein aggregation during grain development: effects of temperatures and water stress. Eur. J. Agron. 16, 1–12.

Dreccer, M.F., Grashoff, C., Rabbinge, R., 1997. Source-sink ratio in barley (*Hordeum vulgare* L.) during grain filling: effects on senescence and grain protein concentration. Field Crops Res. 49, 269–277.

Dreccer, M.F., Slafer, G.A., Rabbinge, R., 1998. Optimization of vertical distribution of canopy nitrogen: an alternative trait to increase yield potential in winter cereals. J. Crop Prod. 1, 47–77.

Dreccer, M.F., Van Oijen, M., Schapendonk, A.H.C.M., Pot, C.S., Rabbinge, R., 2000. Dynamics of vertical leaf nitrogen distribution in a vegetative wheat canopy. Impact on canopy photosynthesis. Ann. Bot. 86, 821–831.

Dubreil, L., Méliande, S., Chiron, H., Compoint, J.-P., Quillien, L., Branlard, G., Marion, D., 1998. Effect of puroindolines on the breadmaking properties of wheat flour. Cereal Chem. 75, 222–229.

Engelen-Eigles, G., Jones, R.J., Phillips, R.L., 2000. DNA Endoreduplication in maize endosperm cells: the effect of exposure to short-term high temperature. Plant Cell Environ. 23, 657–663.

Evers, T., Millar, S., 2002. Cereal grain structure and development: some implications for quality. J. Cereal Sci. 36, 261–284.

Gauch, H.G., Hwang, J.T.G., Fick, G.W., 2003. Model evaluation by comparison of model-based predictions and measured values. Agron. J. 95, 1442–1446.

Gleadow, R.M., Dalling, M.J., Halloran, G.M., 1982. Variation in endosperm characteristics and nitrogen content in six wheat lines. Aust. J. Plant Physiol. 9, 539–551.

Gras, P.W., Anderssen, R.S., Keentok, M., Békés, F., Appels, R., 2001. Gluten protein functionality in wheat flour processing: a review. Aust. J. Agr. Res. 52, 1311–1323.

Graybosch, R.A., Peterson, C.J., Shelton, D.R., Baenziger, P.S., 1996. Genotypic and environmental modification of wheat flour protein composition in relation to end-use quality. Crop Sci. 36, 296–300.

Grindlay, D.J.C., Sylvester-Bradley, R., Scott, R.K., 1995. The relationship between canopy green area and nitrogen in the shoot. In: Lemaire, G., Burns, I.J. (Eds.), Diagnostic Procedures for Crop N Management. Series Les Colloques, vol. 82, INRA Editions. Poitiers, pp. 53–60.

Gupta, R.B., Batey, I.L., MacRitchie, F., 1992. Relationships between protein composition and functional properties of wheat flours. Cereal Chem. 69, 125–131.

Hammond-Kosack, M.C.U., Holdsworth, M., Bevan, M.W., 1993. In vivo footprinting of a low molecular weight glutenin gene (LMWG-1D1) in wheat endosperm. EMBO J. 12, 545–554.

Hwang, Y.-S., Ciceri, P., Parsons, R.L., Moose, S.P., Schmidt, R.J., Huang, N., 2004. The maize O_2 and PBF proteins act additively to promote transcription from storage protein gene promoters in rice endosperm cells. Plant Cell Physiol. 45, 1509–1518.

Jamieson, P.D., Ewert, F., 1999. The role of roots in controlling soil water extraction during drought: an analysis by simulation. Field Crops Res. 60, 267–280.

Jamieson, P.D., Munro, C.A., 2000. The calibration of a model for daylength responses in spring wheat for large numbers of cultivars. Agron. N. Z. 30, 25–29.

Jamieson, P.D., Semenov, M.A., 2000. Modelling nitrogen uptake and redistribution in wheat. Field Crops Res. 68, 21–29.

Jamieson, P.D., Stone, P.J., Semenov, M.A., 2001. Towards modelling quality in wheat—from grain nitrogen concentration to protein composition. Aspects Appl. Biol. 64, 111–126.

Jamieson, P.D., Semenov, M.A., Brooking, I.R., Francis, G.S., 1998a. *Sirius*: a mechanistic model of wheat response to environmental variation. Eur. J. Agron. 8, 161–179.

Jamieson, P.D., Porter, J.R., Goudriaan, J., Ritchie, J.T., van Keulen, H., Stol, W., 1998b. A comparison of the models AFRCWHEAT2, CERES-wheat, Sirius, SUCROS2 and SWHEAT with measurements from wheat grown under drought. Field Crops Res. 55, 23–44.

Jia, Y.Q., Fabre, J.L., Aussenac, T., 1996. Effects of growing location on response of protein polymerization to increased nitrogen fertilization for the common wheat cultivar Soissons: relationship with some aspects of the breadmaking quality. Cereal Chem. 73, 526–532.

Lafiandra, D., Masci, S., Blumenthal, C.S., Wrigley, C.W., 1999. The formation of glutenin polymer in practice. Cereal Foods World 44, 572–578.

Landry, J., 2002. A linear model for quantitating the accumulation of zeins and their fractions ($\alpha+\delta$, β & γ) in developing endosperm of wild-type and mutant maizes. Plant Sci. 163, 111–115.

Lawless, C., Semenov, M.A., Jamieson, P.D., 2005. A wheat canopy model linking leaf area and phenology. Eur. J. Agron. 22, 19–32.

Martre, P., Porter, J.R., Jamieson, P.D., Triboï, E., 2003. Modeling grain nitrogen accumulation and protein composition to understand the sink/source regulations of nitrogen remobilization for wheat. Plant Physiol. 133, 1959–1967.

Müller, M., Knudsen, S., 1993. The nitrogen response of a barley C-hordein promoter is controlled by positive and negative regulation of the GCN4 and endosperm box. Plant J. 4, 343–355.

Niklas, K.J., 1994. Plant Allometry. The Scaling of Form and Process. The University of Chicago Press, Chicago.

Onate, L., Vicente-Carbajosa, J., Lara, P., Diaz, I., Carbonero, P., 1999. Barley BLZ2, a seed-specific bZIP protein that interacts with BLZ1 in vivo and activates transcription from the GCN4-like motif of B-hordein promoters in barley endosperm. J. Biol. Chem. 274, 9175–9182.

Oscarson, P., Lundborg, T., Larsson, M., Larsson, C.M., 1995. Genotypic differences in nitrate uptake and nitrogen utilization for spring wheat grown hydroponically. Crop Sci. 35, 1056–1062.

Panozzo, J.F., Eagles, H.A., Wootton, M., 2001. Changes in protein composition during grain development in wheat. Aust. J. Agr. Res. 52, 485–493.

Pechanek, U., Karger, A., Groger, S., Charvat, B., Schoggl, G., Lelley, T., 1997. Effect of nitrogen fertilization on quality of flour protein components, dough properties, and breadmaking quality of wheat. Cereal Chem. 74, 800–805.

Porter, J.R., 1993. AFRCWHEAT2: a model of the growth and development of wheat incorporating responses to water and nitrogen. Eur. J. Agron. 2, 69–82.

Randall, P.J., Moss, H.J., 1990. Some effects of temperature regime during grain filling on wheat quality. Aust. J. Agr. Res. 41, 603–617.

Shewry, P.R., Halford, N.G., 2002. Cereal seed storage proteins: structures, properties and role in grain utilization. J. Exp. Bot. 53, 947–958.

Shewry, P.R., Tatham, A.S., Halford, N.G., 2001. Nutritional control of storage protein synthesis in developing grain of wheat and barley. Plant Growth Regul. 34, 105–111.

Sinclair, T.R., Amir, J., 1992. A model to assess nitrogen limitations on the growth and yield of spring wheat. Field Crops Res. 30, 63–78.

Singh, B.K., Jenner, C.F., 1982. A modified method for the determination of cell number in wheat endosperm. Plant Sci. Lett. 26, 273–278.

Stone, P.J., Nicolas, M.E., 1996. Varietal differences in mature protein composition of wheat resulted from different rates of polymer accumulation during grain filling. Aust. J. Plant Physiol. 23, 727–737.

Triboï, E., Triboï-Blondel, A.M., 2001. Environmental effects on wheat grain growth and composition. Aspects Appl. Biol. 64, 91–101.

Triboï, E., Martre, P., Triboï-Blondel, A.-M., 2003. Environmentally-induced changes of protein composition for developing grains of wheat are related to changes in total protein content. J. Exp. Bot. 54, 1731–1742.

Tsai, C.Y., Huber, D.M., Warren, H.L., 1980. A proposed role of zein and glutelin as N sinks in maize. Plant Physiol. 66, 330–333.

Uthayakumaran, S., Gras, P.W., Stoddard, F.L., Békés, F., 1999. Effects of varying protein content and glutenin-to-gliadin ratio on the functional properties of wheat dough. Cereal Chem. 23, 33–42.

Vicente-Carbajosa, J., Moose, S.P., Parsons, R.L., Schmidt, R.J., 1997. A maize zinc-finger protein binds the prolamin box in zein gene promoters and interacts with the basic leucine zipper transcriptional activator Opaque2. Proc. Natl. Acad. Sci. U.S.A. 94, 7685–7690.

Weegels, P.L., Hamer, R.J., Schofield, J.D., 1996. Critical review: functional properties of wheat glutenin. J. Cereal Sci. 23, 1–18.

Weir, A.H., Bragg, P.L., Porter, J.R., Rayner, J.H., 1984. A winter wheat crop simulation model without water or nutrient limitations. J. Agric. Sci. 102, 371–382.

Wieser, H., Seilmeier, W., 1998. The influence of nitrogen fertilisation on quantities and proportions of different protein types in wheat flour. J. Sci. Food Agric. 76, 49–55.

Wrigley, C.W., Blumenthal, C., Gras, P.W., Barlow, E.W.R., 1994. Temperature variation during grain filling and changes in wheat grain quality. Aust. J. Plant Physiol. 21, 875–885.

Zhu, J., Khan, K., 2001. Effects of genotype and environment on glutenin polymers and breadmaking quality. Cereal Chem. 78, 125–130.